



Prediction of Dry Sliding Wear Response of AlMg1SiCu/Silicon Carbide/Molybdenum Disulphide Hybrid Composites Using Adaptive Neuro-Fuzzy Inference System (ANFIS) and Response Surface Methodology (RSM)

K. Ragupathy¹ · C. Velmurugan² · D. S. Ebenezer Jacob Dhas³ · N. Senthilkumar⁴ · K. Leo Dev Wins³

Received: 28 September 2020 / Accepted: 4 June 2021 / Published online: 23 June 2021
© King Fahd University of Petroleum & Minerals 2021

Abstract

In this research work, an effort was made to predict the dry sliding wear response of AlMg1SiCu alloy hybrid composites which were reinforced with 10% Silicon carbide particles (SiC) together with weight fractions of 3, 6 and 9% of self-lubricant molybdenum disulphide particles (MoS₂) through melt stir casting. The wear behaviour of the hybrid composite samples was evaluated based on Box-Behnken design on pin-on-disc tribometer without lubrication. The output response weight loss was employed to train the neural network model in ANFIS back-propagation algorithm. The weight loss of 9% MoS₂ hybrid composite reduced at low sliding speeds, due to the development of shallow sliding grooves and MoS₂-lubricated tribolayer. Scanning electron micrographs and EDS of the AlMg1SiCu alloy hybrid composites revealed a uniform distribution of SiC and MoS₂ particles. The tensile strength of the as-cast hybrid composites increases as the wt.% of MoS₂ particles increases, according to the tests. However, the addition of MoS₂ improved the hardness of the hybrid composites until it reached 6 wt.%, after which it decreased slightly. Weight loss and coefficient of friction decreased by addition of self-lubricant MoS₂ in the matrix material. Worn-out surface of the hybrid composite shows the controlling wear mechanisms of the composites, and well-trained ANFIS model could accurately predict the responses better when compared with the response surface methodology model.

Keywords Aluminium hybrid composites · Silicon carbide · Molybdenum disulphide · RSM · ANFIS

1 Introduction

AlMg1SiCu alloy plays an important role in the fabrication of hybrid aluminium metal matrix composites (MMCs) and it is widely utilized in all types of manufacturing and research fields owing to their high strength-to-weight ratio,

high stiffness, good wear resistance and low coefficient of thermal expansion. AlMg₁SiCu alloy could be reinforced with ceramics particles in order to improve its specific physical properties. Rao and Das [1] observed that inclusion of SiC particles in the aluminium alloys decreases wear rate and the wear rate of Aluminium 10 wt.% SiC composite was minimal. Several materials have seen their wear-resistant properties improved by using solid lubricants such as MoS₂ and graphite. The wear performance of silicon carbide particles (SiC) reinforced with aluminium alloys with various volume percentage was investigated by Bauri and Surappa [2].

The wear resistance increases in metal matrix composites (MMCs) due to inclusion of 5 wt.% graphite particles with aluminium alloy 6061 and boron carbide (B₄C) particles. The addition of graphite particles plays a key role in decreasing the wear of these composites [3]. Earlier research [4] reported that Al–Si10Mg alloy reinforced with 2 and 4%

✉ K. Ragupathy
ragupathy86@gmail.com

¹ Adhiparasakthi Engineering College, Tamil Nadu, Melmaruvathur 603319, India

² Kumaraguru College of Technology, Tamil Nadu, Coimbatore 641049, India

³ Karunya Institute of Technology and Sciences, Tamil Nadu, Coimbatore 641114, India

⁴ Saveetha School of Engineering, Saveetha Institute of Medical and Technical Sciences, Tamil Nadu, Chennai 602105, India



Table 1 Compositions of the hybrid composites

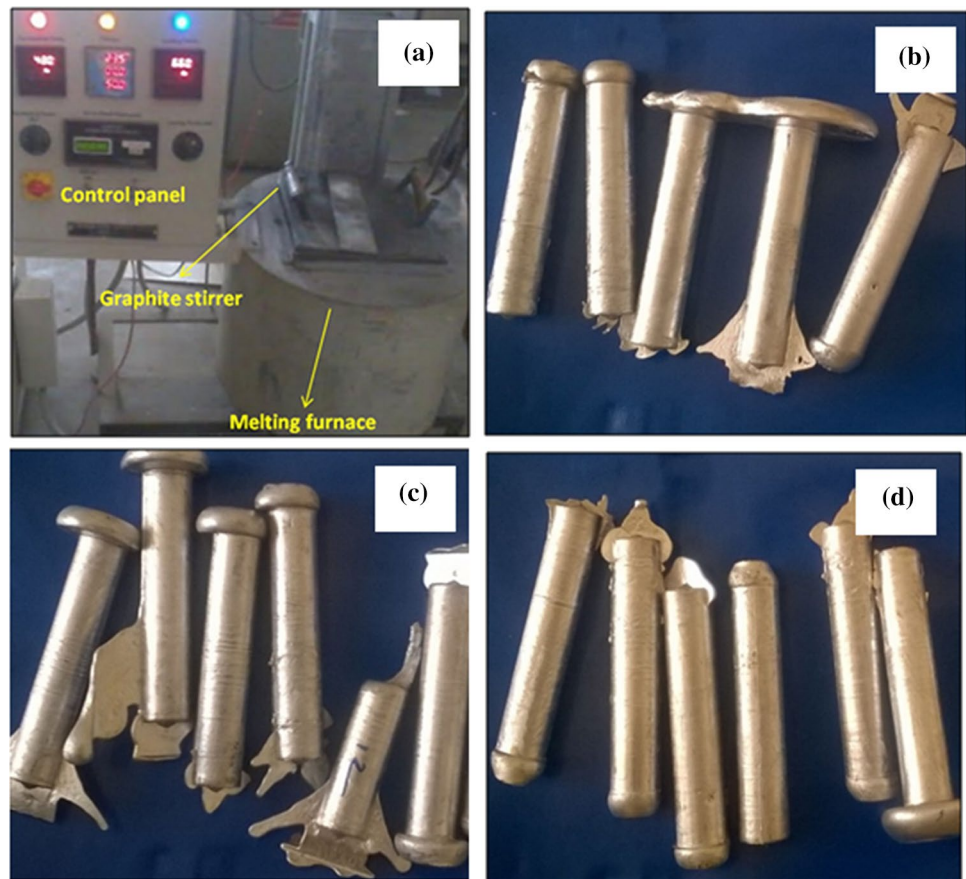
Sample No.	Specimen composition
1	AlMg1SiCu + 10% SiC + 3% MoS ₂
2	AlMg1SiCu + 10% SiC + 6% MoS ₂
3	AlMg1SiCu + 10% SiC + 9% MoS ₂

of MoS₂ was fabricated through the stir casting route. The presence of MoS₂ composites exhibits an enormous change in wear rate. There are many techniques available for fabrication of aluminium hybrid metal matrix composites like spray, chemical vapour deposition, powder-metallurgy, infiltration process and in situ reaction processing along with the

melt stir casting route. Compared to all types of production routes, the melt stir casting method is the most economical and follows a well-known simplest technique to attain uniform distribution of the reinforcement particles. Graphite particles known for their self-lubrication properties, when reinforced with aluminium alloys have been effectively wetted using the melt stir casting route [5].

So as to enhance the wear properties of the monolithic MMCs, solid reinforcements such as molybdenum disulphide (MoS₂), tungsten disulphide (WS₂) and graphite (Gr) are used. In dry conditions, it has been demonstrated that the MoS₂ particles perform better than Gr particles as a solid lubricant [6].

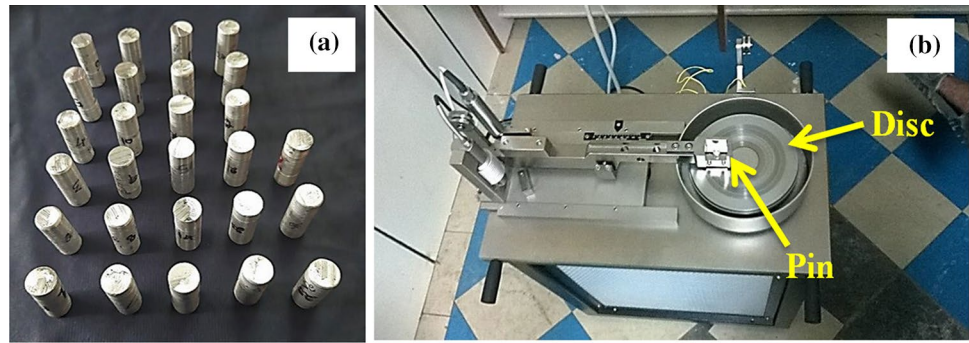
Fig. 1 **a** Stir casing set-up, **b** as-cast AlMg1SiCu + 10% SiC + 3% MoS₂ hybrid composite, **c** as-cast AlMg1SiCu + 10% SiC + 6% MoS₂ hybrid composite, **d** as-cast AlMg1SiCu + 10% SiC + 9% MoS₂ hybrid composite

**Table 2** Experimental levels of the input parameters

Process parameters	Levels					
	Un-coded	Coded	Units	Low (−1)	Medium (0)	High (+)
Weight fraction of MoS ₂ particles	A	X ₁	wt.%	3	6	9
Speed	B	X ₂	rpm	200	300	400
Applied load	C	X ₃	kg	1	2	3
Sliding distance	D	X ₄	m	300	600	900



Fig. 2 a Worn-out hybrid composite samples; **b** pin-on-disc tribometer



The tribological behaviour of Al–Al₂O₃–MoS₂ composites which slide against the EN 32 counter face were statistically analysed by Dharmalingam et al. [7] and found that the friction coefficient and specific wear rate are strongly affected by the inclusion of MoS₂ particles. The composites

of Al–Al₂O₃–MoS₂ were produced through the technique of stir casting.

Monikandan et al. [8] have investigated the wear behaviour of AA6061-10 wt.% virgin composites of B₄C–MoS₂ reinforced with 2.5, 5 and 7.5 wt.%. The microstructural analysis of the hybrid composites showed uniform

Table 3 Box-Behnken experimental design

Runs	X ₁ (%)	X ₂ (rpm)	X ₃ (kg)	X ₄ (m)	Weight loss (g)			Coefficient of friction
					Experimental value	Predicted value	Residual	
1	3 (-1)	300 (0)	1 (-1)	600 (0)	0.23	0.21	0.02	0.408
2	3 (-1)	300 (0)	2 (0)	300 (-1)	0.18	0.15	0.03	0.425
3	3 (-1)	200 (-1)	2 (0)	600 (0)	0.35	0.35	0.00	0.437
4	3 (-1)	400 (+1)	2 (0)	600 (0)	0.32	0.34	-0.02	0.411
5	3 (-1)	300 (0)	2 (0)	900 (+1)	0.58	0.56	0.02	0.429
6	3 (-1)	300 (0)	3 (+1)	600 (0)	0.41	0.43	-0.02	0.466
7	6 (0)	300 (0)	1 (-1)	300 (-1)	0.11	0.12	-0.01	0.314
8	6 (0)	200 (-1)	1 (-1)	600 (0)	0.33	0.32	0.01	0.328
9	6 (0)	300 (0)	1 (-1)	900 (+1)	0.52	0.53	-0.01	0.308
10	6 (0)	400 (+1)	1 (-1)	600 (0)	0.30	0.31	-0.01	0.254
11	6 (0)	300 (0)	2 (0)	600 (0)	0.46	0.49	-0.03	0.334
12	6 (0)	200 (-1)	2 (0)	300 (-1)	0.18	0.20	-0.02	0.348
13	6 (0)	400 (+1)	2 (0)	300 (-1)	0.30	0.28	0.02	0.327
14	6 (0)	200 (-1)	2 (0)	900 (+1)	0.63	0.63	0.00	0.345
15	6 (0)	400 (+1)	2 (0)	900 (+1)	0.67	0.64	0.03	0.331
16	6 (0)	300 (0)	3 (+1)	900 (+1)	0.73	0.73	0.00	0.367
17	6 (0)	300 (0)	3 (+1)	300 (-1)	0.38	0.36	0.02	0.359
18	6 (0)	200 (-1)	3 (+1)	600 (0)	0.49	0.49	0.00	0.371
19	6 (0)	400 (+1)	3 (+1)	600 (0)	0.58	0.58	0.00	0.349
20	6 (0)	400 (+1)	3 (+1)	300 (-1)	0.38	0.39	-0.01	0.356
21	6 (0)	300 (0)	2 (0)	600 (0)	0.51	0.49	0.02	0.253
22	9 (+1)	300 (0)	1 (-1)	600 (0)	0.29	0.26	0.03	0.241
23	9 (+1)	300 (0)	2 (0)	300 (-1)	0.19	0.21	-0.02	0.259
24	9 (+1)	200 (-1)	2 (0)	600 (0)	0.35	0.34	0.01	0.233
25	9 (+1)	400 (+1)	2 (0)	600 (0)	0.44	0.44	0.00	0.264
26	9 (+1)	300 (0)	2 (0)	900 (+1)	0.56	0.59	-0.03	0.278
27	9 (+1)	300 (0)	3(+1)	600 (0)	0.53	0.51	0.02	0.339

reinforcement dispersion (MoS_2 and B_4C). The hardness of the composites steadily decreased as the amount of MoS_2 particles added increased. The results also shown that decrease in wear rate of the composite material could be observed up to a sliding speed of 2 m/s, due to the formation of MoS_2 tribolayer, after which wear rate increases, since the tribolayer disintegrates leading to abrasion and delamination. High wear-resistant materials contain strong tribolayer on the wear surface and form fine equi-axed wear fragments under dry environment. Wear mechanisms are system-dependent, and wear parameters basically rely on composition of material, load applied, grain size, hardness, sliding speed and environmental conditions [9].

Prasanta Sahoo and Shouvik Ghosh have carried out wear tests on pin-on-disc tester and in their investigations they selected various factors namely volume fraction, sliding distance, speed and applied load [10]. During the wear experiments, the wear rate was measured as an output response

parameter and the wear of samples depends on the input parameters which are reinforcement weight fraction, sliding distance, applied load, speed, reinforcement particle size and type. The relationship between input parameters and wear rate has been determined through some statistical and numerical techniques. The majority of the researchers' preferred Taguchi method and applied factorial design method to examine the wear characteristics of aluminium hybrid composites [11–13]. The statistical approach such as RSM allows determining the input parameter–output response relationships more accurately. In RSM technique, most of researchers utilize the central composite design for dry sliding wear on MMCs [14]. However, nonlinear modelling of wear prediction of aluminium hybrid composites using Box-Behnken design has been reported rarely.

Manjunath et al. [15] studied that input–output relationships in Box-Behnken design (BBD) and central composite design (CCD) models on wear performance of squeeze cast

Fig. 3 a ANFIS general structural design, b complete structure of ANFIS design for trained weight loss model

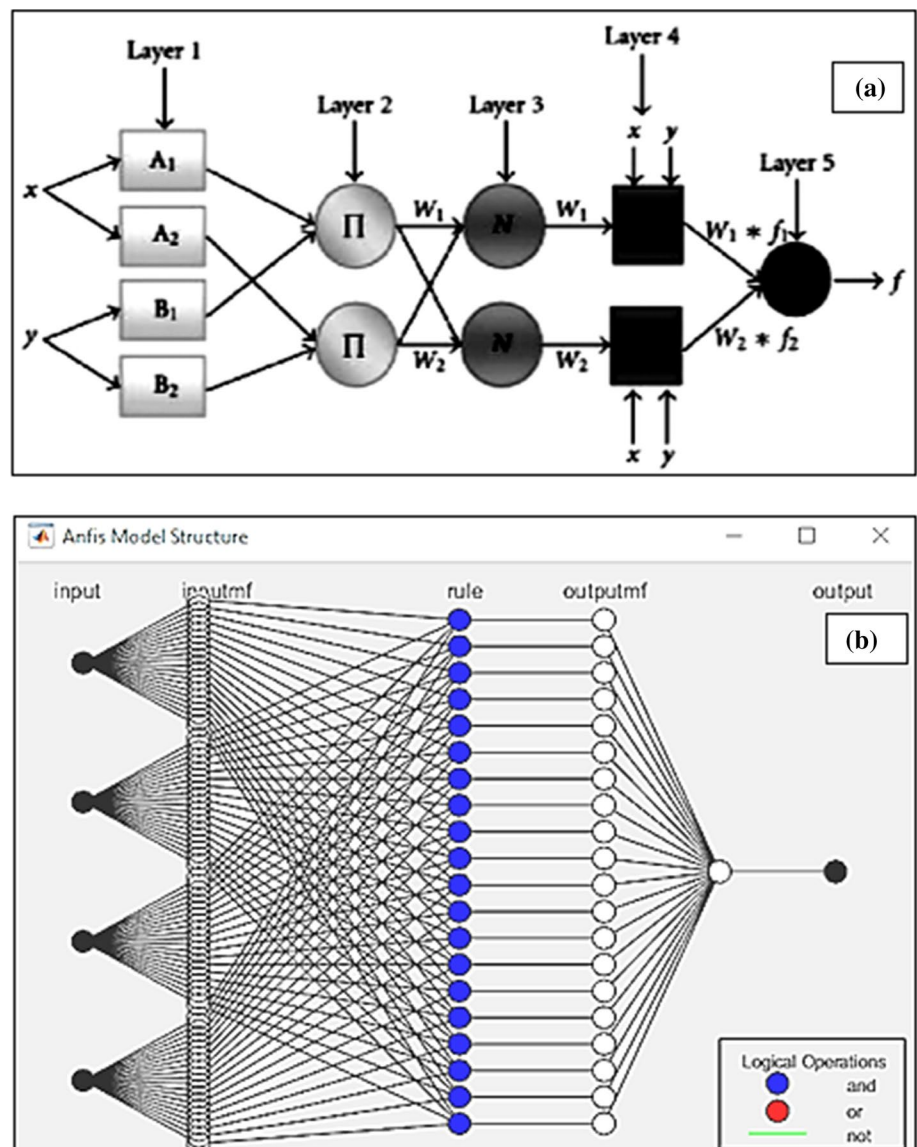


Table 4 Error functions and its equations

Error function	Equation
Root mean square error	$RMSE = \frac{\sqrt{\sum_{i=1}^n (Y_{i,e} - Y_{i,p})^2}}{n}$
Mean absolute error (%)	$MAE = \frac{1}{n} \sum_{i=1}^n Y_{i,e} - Y_{i,p} $
Standard error of prediction (%)	$SPE (\%) = \frac{RMSE}{Y_{i,e}} \times 10$
Model predictive failure (%)	$MEP (\%) = \frac{100}{n} \sum_{i=1}^n \frac{ Y_{i,e} - Y_{i,p} }{Y_{i,p}}$
Coefficient of determination (R^2)	$R^2 = \frac{\sum_{i=1}^n (Y_{i,p} - Y_{i,e})}{\sum_{i=1}^n (Y_{i,p} - Y_e)^2}$
Chi-square statistic (χ^2)	$\chi^2 = \sum_{i=1}^n \frac{(Y_{i,p} - Y_{i,e})^2}{Y_{i,p}}$

aluminium hybrid composites. The result revealed that Box-Behnken design was superior to the CCD model in predicting the density of casting. Most of the literature focused on the CCD models for predicting wear performance of

aluminium hybrid composites. ANFIS is a fuzzy system of inference that can be used in models of neural networks to predict the wear loss of Al–SiC composite [16]. RSM was used to develop the mathematical model. The model’s input factors are wt.% of reinforcement, particle size, load, sliding speed and sliding distance, whereas wear loss of Al–SiC MMCs was considered as the output response. The experimental data were compared with the ANFIS model. The performance of wear rate prediction of Al–SiC MMCs by ANFIS model was found to be effective. Velmurugan et al. [17] predicted the volume loss of heat treated aluminium alloy 6061 metal matrix composites, fabricated by stir casting process, using the ANN method. The results indicated that the constructed mathematical model is consistent and precise in predicting the volume loss.

In a recent study, an L_{16} orthogonal array was built using Taguchi design and a hybrid grey relational analysis combined with RSM was employed to design the experiments. The coefficient of friction, wear rate of pin and frictional

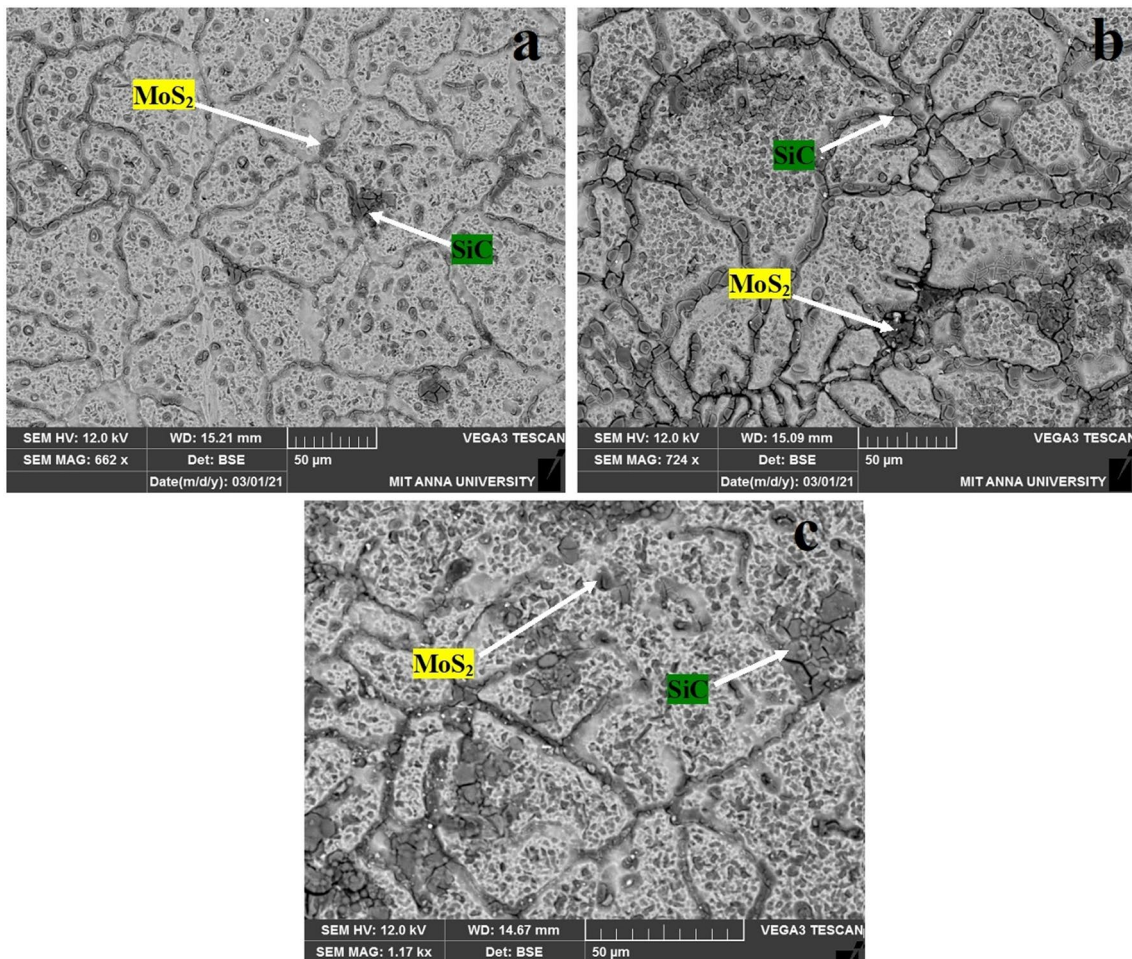


Fig. 4 a–c Microstructure of the samples; **a** SEM image of 3 wt.% MoS₂ hybrid composite, **b** SEM image of 6 wt.% MoS₂ hybrid composite

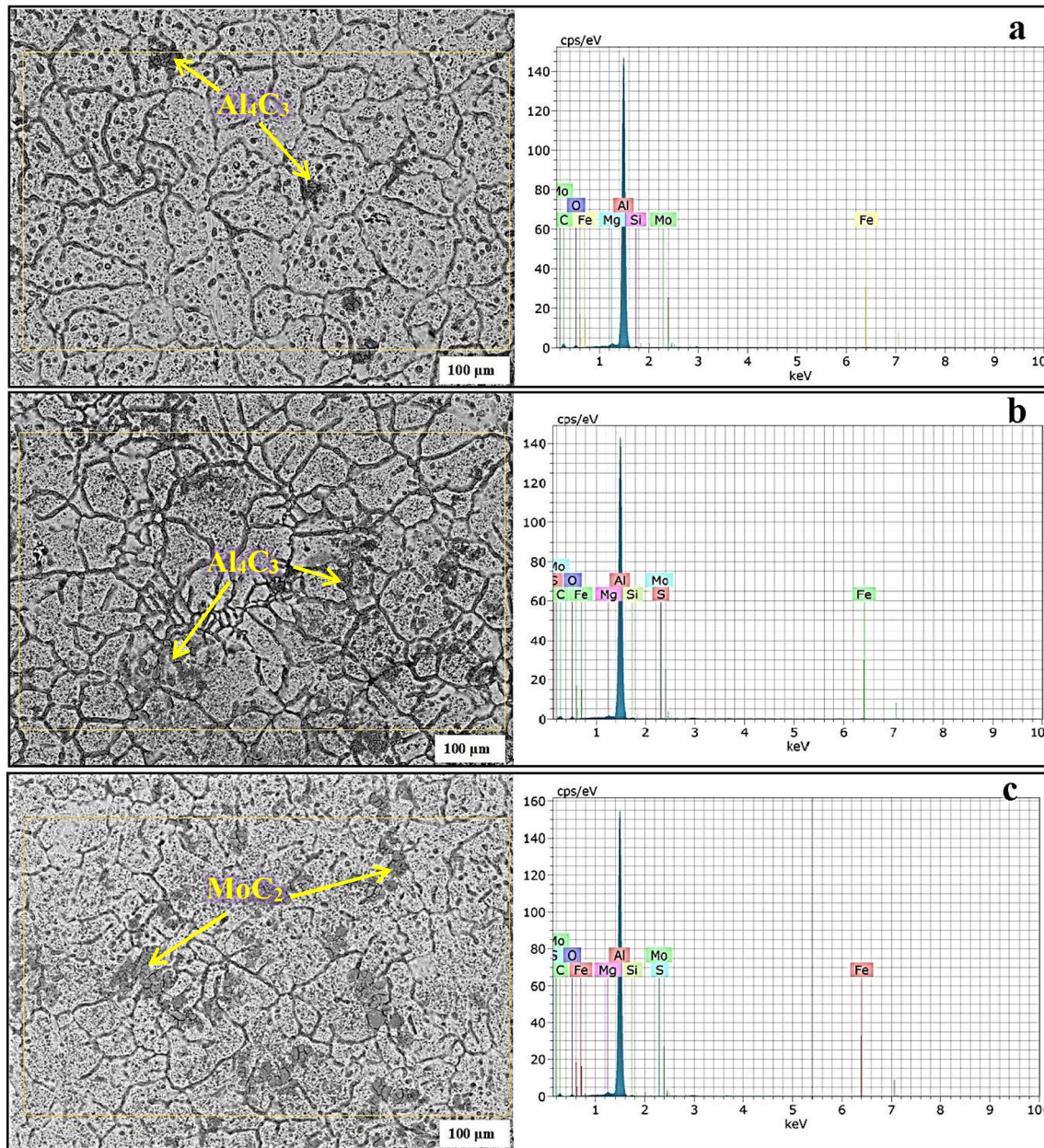


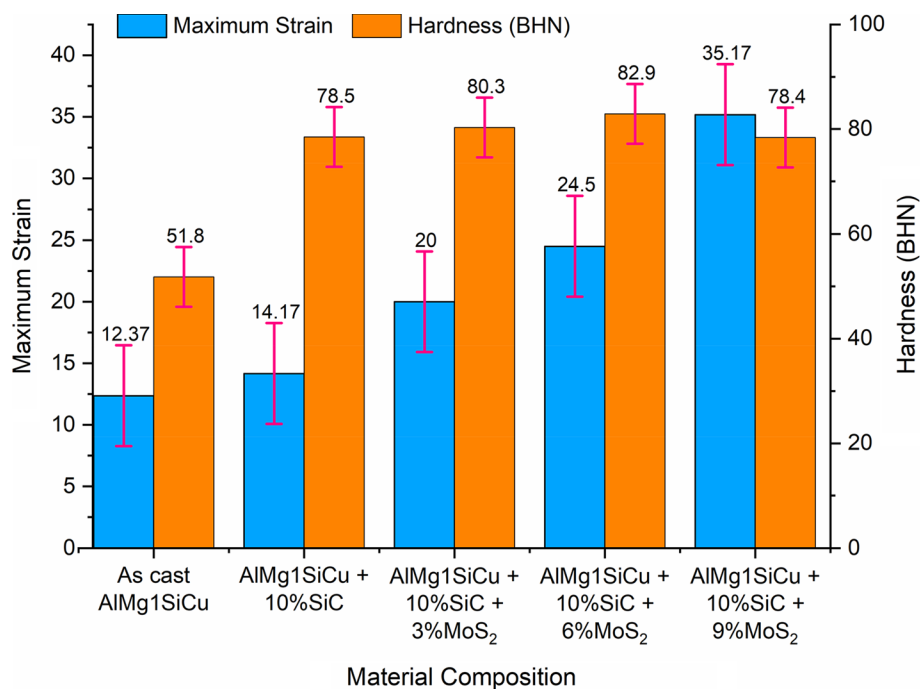
Fig. 5 a–c SEM micrograph and EDS plot of **a** 3 wt.% MoS₂ hybrid composite, **b** 6 wt.% MoS₂ hybrid composite, **c** 9 wt.% MoS₂ hybrid composite, highlighting the presence of intermetallic phases that were formed after the stir casting process

force were considered for analysis and the optimal setting of the experiments was predicted, through the analysis [18].

The objective of the current study is to compare the models of RSM and ANFIS to predict the weight loss of stir cast AA6061/10% SiC/3%, 6% and 9% MoS₂ hybrid composites and to compare the effectiveness of the RSM and ANFIS models. Based on the literature, SiC weight fraction was held constant at 10%, in order to improve mechanical properties and different weight fractions of MoS₂ (3, 6 and 9%) were selected for the present study in order to find the effect of wt.% of MoS₂ particles on the weight loss of the hybrid

composites [8, 12]. It is decided to conduct the experimental runs using Box-Behnken experimental design to record the weight loss corresponding to the input parameters such as percentage of reinforcement (3, 6 and 9% MoS₂), sliding distance (300, 600 and 900 m), applied load (1, 2 and 3 kg) and speed (200, 300 and 400 rpm). Apart from optimization techniques, a thorough investigation about the under lying mechanisms behind the wear behaviour, mechanical properties, worn-out surface morphology and distribution of reinforcements in the matrix of the hybrid composites are also proposed. Very limited papers are available in modelling

Fig. 6 Hardness and maximum strain of as-cast AlMg1SiCu alloy and hybrid composites



the dry sliding wear response of the aforementioned hybrid composites (which includes molybdenum disulphide) compared to other solid lubricants.

2 Experimental Work

2.1 Materials and Stir Casting

The continuous phase used for the hybrid MMCs in the present work is aluminium alloy AlMg1SiCu. These cast alloys are mostly used in aerospace and structural applications due to their corrosion resistance and cast-ability. Silicon carbide (SiC) and molybdenum disulphide (MoS₂) particles were added into the matrix material to increase the hardness, wear resistance and lubricity. The stir casting method was chosen for the fabrication of the aluminium hybrid composites in which preheated reinforcing materials such as silicon carbide and molybdenum disulphide were included into the molten matrix pool with the use of a mechanical stirrer. In order to control accumulation of SiC and MoS₂ particles, impeller position of the stirrer was kept at about one third of the height of the melt from the bottom of the crucible. The molten matrix alloy was stirred for time duration of about 10 min by the action of the stirrer. The speed of the mechanical stirrer was kept at 600 rpm. The molten melt was transferred to the cast iron moulds at 600 °C. This method is similar to the composite fabrication route preferred by previous researchers [19, 20]. The compositions of the fabricated aluminium hybrid composites are shown in Table 1. The

photographs of the stir casting set-up and cast samples for different composition are shown in Fig. 1a–d.

2.2 Wear Tests

Box-Behnken design (BBD) was used to design the wear experiments. The input parameters are weight fraction of MoS₂ particles (X_1), speed (X_2), applied load (X_3) and sliding distance (X_4). Their corresponding levels used in this investigation are given in Table 2.

Each input parameter was varied at three different levels ($-1, 0, +1$). After fabrication of cast hybrid composites, test samples with 10 mm diameter and 30 mm length were machined for wear studies as shown in Fig. 2a. Dry sliding wear tests were performed as per ASTM G99-95 standard using a pin-on-disc tribometer as shown in Fig. 2b. The test runs were performed by rubbing the test specimen against a rotating disc of EN-32 steel with surface roughness, R_a 0.1 and having hardness of 63 HRC under dry conditions [18, 21].

Before testing, the samples and the disc surface were cleaned with acetone. The weights of the specimens were measured to calculate the wear loss. Due to wide range of parameters, it was planned to take the common input parameters like speed, applied load, sliding distance and weight fraction of the reinforcements. The tests were conducted [13] at a relative humidity of 30% and ambient temperature of 30 °C, with three trials and the average test result was taken for weight loss from the pin-on-disc tester. The input levels of wear parameter design matrix and corresponding responses are given in Table 3.

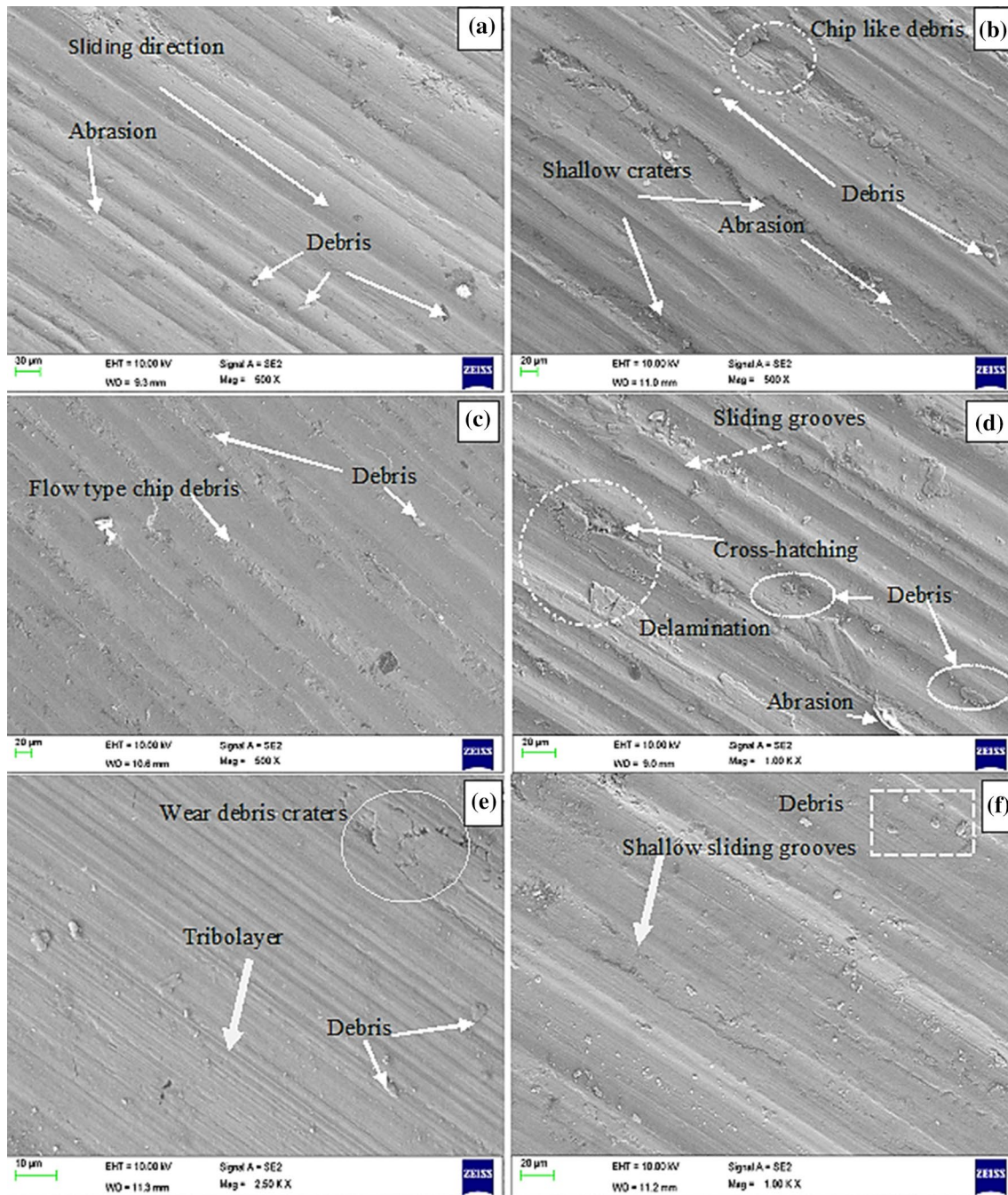


Fig. 7 **a–c** Tensile strength and elasticity modulus of as-cast AlMg1SiCu alloy and hybrid composites, **b** stress strain curves of as-cast AlMg1SiCu alloy and hybrid composites, **c** SEM image of 9 wt.% MoS₂ hybrid composite

2.3 Hardness Test

The hybrid metal matrix composite specimens were polished using abrasive sheets of standard grit sizes (400–1000). Hardness was measured using a Brinell hardness tester for both mono and hybrid metal matrix composite specimens. A test force of 500 kg was applied using the carbide ball

indenter for a period of 15 s at five different positions on the surface of the specimens as per ASTM E10-18 [22].

2.4 Tensile Test

According to ASTM E8 standard, tensile test was carried out at ambient conditions on the test samples of diameter of 10 mm and a gauge length of 60 mm using an automated

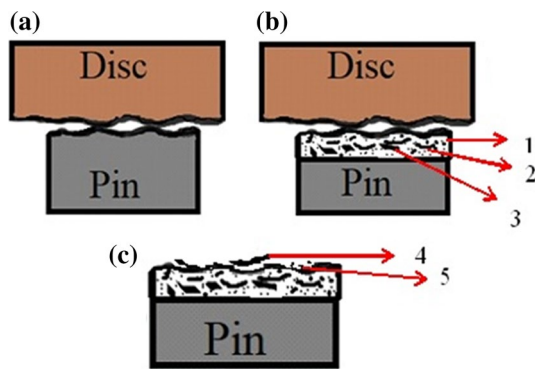


Fig. 8 a-f Worn-out surface morphology of: **a** 3% MoS₂ hybrid composite applied with load 1 kg, **b** 3% MoS₂ hybrid composite applied with load 3 kg, **c** 6% MoS₂ hybrid composite applied with load 1 kg, **d** 6% MoS₂ hybrid composite applied with load 3 kg, **e** 9% MoS₂ hybrid composite applied with load 1 kg, **f** 9 wt.% of MoS₂ hybrid composite applied with load 3 kg

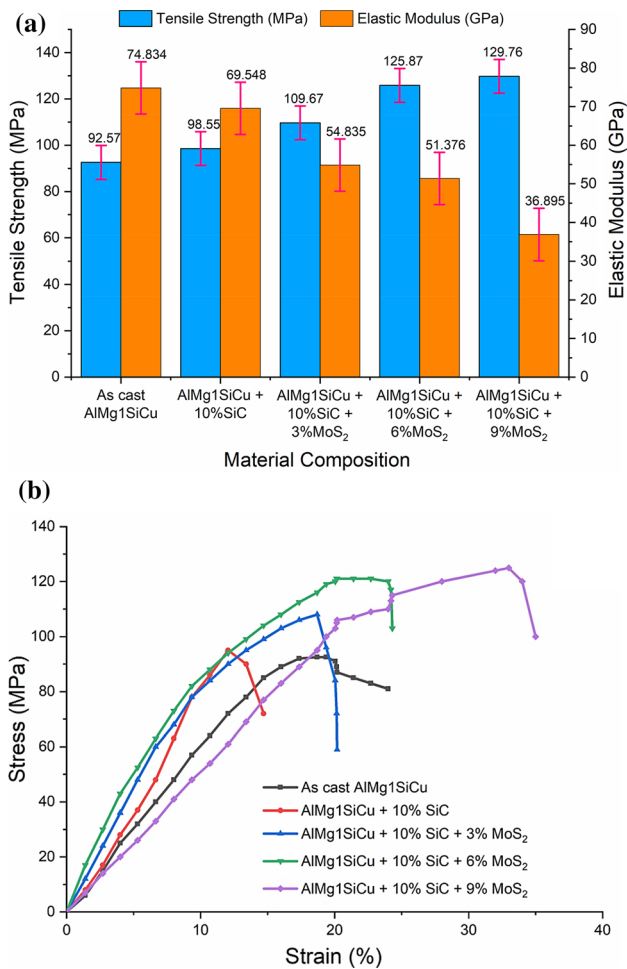


Fig. 9 Schematic diagrams showing the mechanism of delamination and wear debris formation. **a** Contact of pin (wear sample) and disc surface, **b** formation of MoS₂ lubricated tribolayer consisting of 1. AlMg1SiCu alloy, 2. SiC, 3. MoS₂, **c** 4. Platelet-shaped delaminated debris and 5. Micro-cracks on SiC particles

servo system. To reduce the machining marks and their effects on the specimen, the test specimens were prepared by rubbing on SiC emery sheet of 1200 grit size.

2.5 Micro Structural Evaluation

Scanning electron microscopy was used to examine the distribution of particulates within the matrix. The Keller’s reagent was applied as the etchant on the samples to expose the grain boundaries of the composite at micron level. JOEL scanning electron microscope (Model: JSM 6390) was used to observe the microstructure.

2.6 Mathematical Modelling Using Response Surface Methodology

In this work, RSM was used to evaluate the direct and combined influence of weight fraction of MoS₂ (X_1), speed (X_2), applied load (X_3), and sliding distance (X_4) as independent variables on the weight loss of the aluminium hybrid composites. The weight loss is the dependent variable of the hybrid composites, which is to be optimized. The values of the input variables were translated to a coded value of x_i for the statistical technique using Eq. 1.

$$x_i = \frac{X_i - X_0}{\Delta X_1} \tag{1}$$

where

The actual values of an input variable, the output response variable at the centre point and the phase shift value are represented by x_i , x_0 , and Δx_1 , respectively. Table 2 shows the levels of the parameters. Small, moderate, and high coded values for each parameter were labelled as -1 , 0 and $+1$, respectively.

Twenty-seven experimental runs were designed and are presented in Table 3. A second-order polynomial was employed to fit the output response and to derive the mathematical correlation of the input parameters and the output response as per Eq. 2 [30].

$$Y = \beta_0 + \sum_{i=1}^k \beta_i x_i + \sum_{i=1}^k \beta_{ii} x_i^2 + \sum_{i=1}^{k-1} \sum_{j=2}^k \beta_{ij} x_i x_j + \epsilon \tag{2}$$

where

Y is the predicted output response (weight loss), β_0 is the model constant and β_i , β_{ii} and β_{ij} are linear coefficient, quadratic coefficient and interaction coefficient, respectively. x_i and x_j are input parameters, where i and j are the index numbers and $i < j$ condition should be considered for $(x_i x_j)$ interaction term. The k is the number of factors and ϵ represents the statistical error.

Table 5 ANOVA results

ANOVA for response surface quadratic model—analysis of variance table						
Source	Sum of squares	Dof	Mean squares	F Value	p-value	Prob > F
Model	0.674289	14	0.048163	62.61907	<0.0001	Significant
A-composition	0.005586	1	0.005586	7.262574	0.0195	
B-speed	0.003201	1	0.003201	4.161934	0.0640	
C-load	0.017636	1	0.017636	22.92952	0.0004	
D-distance	0.010795	1	0.010795	14.03531	0.0028	
AB	0.0036	1	0.0036	4.680489	0.0514	
AC	0.0009	1	0.0009	1.170122	0.3006	
AD	0.000225	1	0.000225	0.292531	0.5985	
BC	0.003104	1	0.003104	4.035118	0.0676	
BD	0.001193	1	0.001193	1.550414	0.2368	
CD	0.000573	1	0.000573	0.74538	0.4049	
A ²	0.037012	1	0.037012	48.12009	<0.0001	
B ²	0.004165	1	0.004165	5.415538	0.0383	
C ²	0.005677	1	0.005677	7.38148	0.0187	
D ²	0.001618	1	0.001618	2.103014	0.1726	
Residual	0.00923	12	0.000769			
Lack of fit	0.00798	11	0.000725	0.580349	0.7840	Not significant
Pure error	0.00125	1	0.00125			
Corr. total	0.683519	26				

The ANOVA was performed to identify significant factors in a developed model. The main purpose of ANOVA was to categorize the key factors and to identify the most significant factor and also if the experiment results are adequate. If *p*-value of a factor is less than 0.05, the factor is considered to be significant [7, 12, 15]. Design-Expert software (8.0.7.1) was used for mathematical modelling.

2.7 Adaptive Neuro-Fuzzy Inference System (ANFIS)

ANFIS is a fuzzy interrelated inference method which is applied to the framework of an adaptive neural network. From ANFIS general structural design (Fig. 3a), it is examined that the given values of the principle parameters, on the whole output function, can be addressed as a linear grouping of the resulting parameters. Based on this information a hybrid learning rule is taken here, which will come together as a gradient descent and the least squares method is used to find out the precursor parameters. The complete structure of ANFIS design for trained model is shown in Fig. 3b [24].

2.8 Comparison of RSM and ANFIS models

The prediction accuracy and fitting of the developed models were evaluated by analyses of model predictive error (MPE), standard error of prediction (SEP), root mean square error (RMSE), mean absolute error (MAE), coefficient of determination (R^2) and Chi-square statistic (χ^2) between

experimental and predicted data. The error functions and their equations are listed in Table 4.

3 Results and Discussion

3.1 Microstructural Analysis

Figure 4a–c shows the dispersion of reinforcement particles in the AlMg1SiCu hybrid composites [7, 10, 23]. The melting point of SiC particles is very high compared with base material, and hence, they are partially solidified in the base material and appear as small plate-like structure. In addition to that, secondary ceramic strengthening particulates such as MoS₂ (soft materials) are used as lubricants to enhance the wear properties. The matrix phase is α -phase which comprises of the Al/SiC composition, and the SiC particles were found to resemble small plate-like structure. The secondary phase is β -phase (MoS₂ particles), which are found to be globular in nature. Due to that reduction in grain refinement has been observed and hence the mechanical properties increases significantly. No agglomeration of SiC and MoS₂ particles in the mixture could be observed from the micrographs. Also, the MoS₂ and SiC particles were identified based on the backscattered electron micrograph. The image reveals uniform mixture of aluminium, silicon carbide and molybdenum disulphide over the AlMg1SiCu matrix [31, 32].

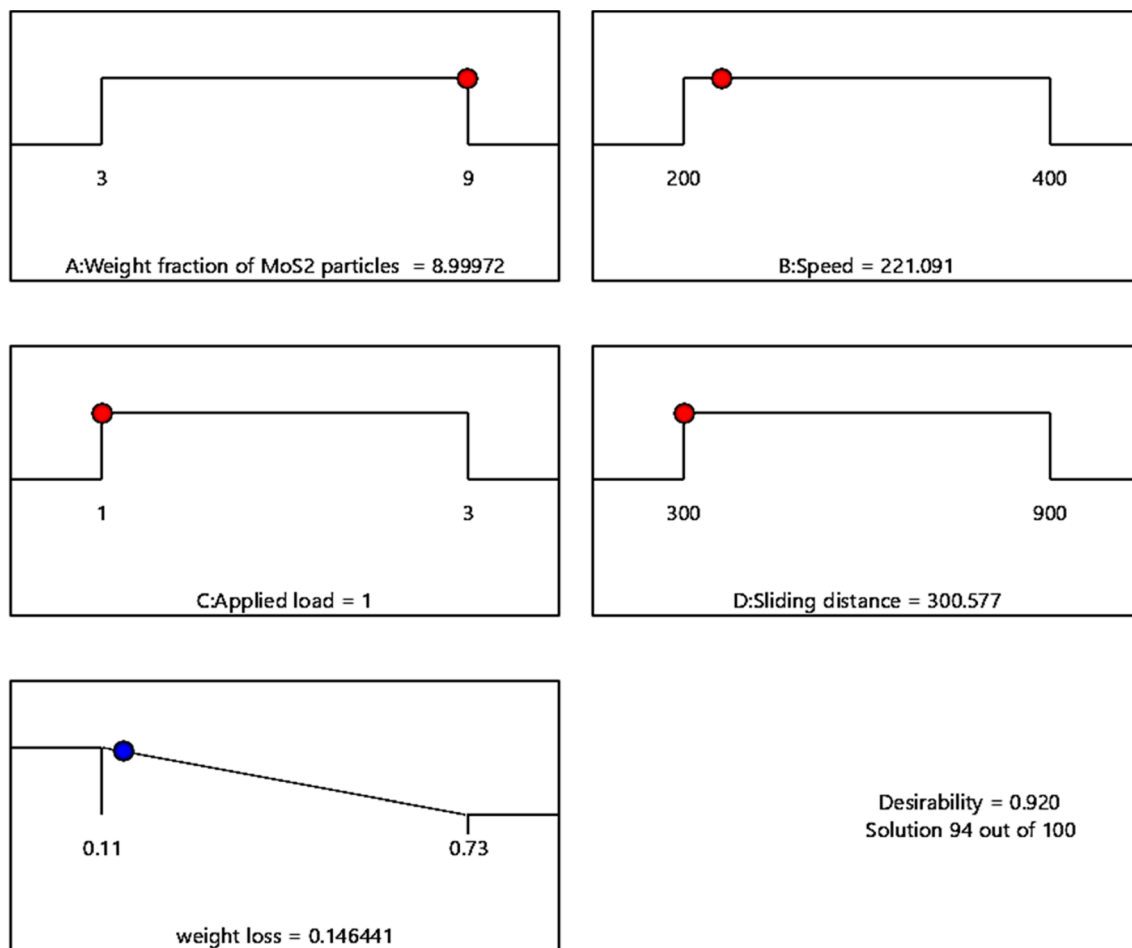


Fig. 10 Desirability ramp function plot for weight loss of hybrid composites

The surface EDS of the AlMg1SiCu/silicon carbide/molybdenum disulphide composite samples is shown in Fig. 5a–c. High intensity peaks are observed for aluminium and its functional elements such as molybdenum, silicon, manganese, magnesium and iron. The additional impurities such as oxygen, nitrogen and carbon are recorded with low peaks. EDS elemental plot endorses the presence of aluminium, silicon, molybdenum and sulphur. The different phases formed during stir casting were identified from the EDS spot analysis. Intermetallic phases such as Al_4C_3 and MoC_2 were observed within the AlMg1SiCu matrix.

3.2 Hardness

Figure 6 indicates the influence of wt.% of reinforcements on the hardness of the different composite samples. It is observed that hardness of the reinforced composites is greater than the hardness of the base alloy and it steadily increases with increasing addition of reinforcement particles up to 9 wt.% of MoS_2 and further decreases upon addition of MoS_2 particles, but the strain value of the composite

specimens steadily increases with the increase in addition of MoS_2 . The lubrication property is due to the addition of particles. Particles of MoS_2 stimulate fast grain movement along the slip planes, thereby causing the sample to deform freely beneath the indenter [20].

3.3 Worn-out Surface Morphology

Scanning electron microscopic analysis was used to study the worn-out surfaces and to reveal the wear mechanisms involved in the AlMg1SiCu/silicon carbide/molybdenum disulphide hybrid composites. Figure 7a and b illustrates the worn-out surface of 3% MoS_2 composites while applying with 1 kg and 3 kg loads, respectively. During sliding, the removal of material occurs on the contact surface of the pin, in the form of plate-shaped particles, resulting in the development of shallow craters with grooves across its surface. When the worn-out surface of 6% MoS_2 composites was applied with a load of 3 kg (Fig. 7c) along with rise in sliding speed, small debris was produced. The detached particles (shown as dotted circle) are observed on the contact

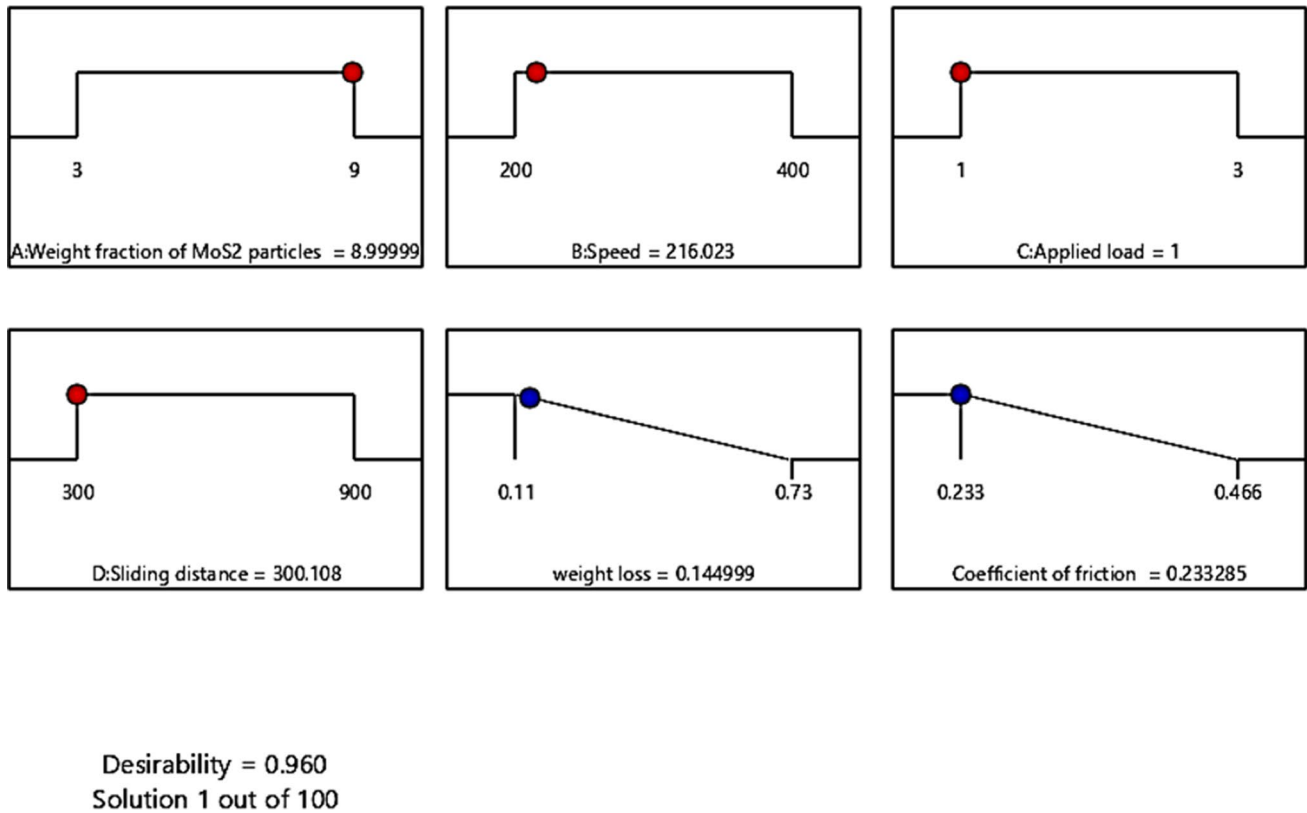


Fig. 11 Desirability ramp function plot for coefficient of friction of hybrid composites

surface of the sample. Because of this wear mechanism, the propagation of the crack could be observed as shallow sliding grooves (shown with dotted arrow) (Fig. 7d). With the increase in sliding speed, abrasion marks on the worn pin surface may also be seen. The abrasion caused cross-hatching and heavy damage (shown with an arrow) on the surface of the worn pin during maximum load condition at 3 kg. With the development of these cross-hatchings, platelet-shaped delaminated debris was formed.

While sliding, the plastic deformation at the subsurface makes the MoS₂ particles to stick to the worn-out surface of the pin and develops micro-cracks on SiC particles which ultimately causes them to break into fine particles. Sannino and Rack [25] observed similar type of cracking in ceramic particulates in their work, for a standard tribo-couple during sliding. In Fig. 7e–f, a tribolayer could be perceived on the worn-out surface of 9% MoS₂ composites. MoS₂ particles crushed, smudged and mixed with debris on the surface of contact are then moved backward and forward between the tribo-couple with debris results in the formation of MoS₂-lubricated tribolayer [7] which results in the absence of delamination or adhesion, but shallow grooves along the direction of sliding on the worn-out surface. Smoother worn-pin surface was attained for 9% MoS₂ hybrid composite, because of the shallow sliding grooves as shown in

Fig. 7f. The weight loss of the hybrid composite at low sliding speeds is significantly lesser due to the MoS₂-lubricated tribolayer formation, but at high sliding speeds, delamination and abrasion wear mechanisms are being induced [8, 23–28].

Also, the AlMg₁SiCu/silicon carbide/molybdenum disulphide hybrid composites with the increase in sliding speed exhibited a decrease in the coefficient of friction due to the presence of MoS₂-lubricated tribolayer (solid lubricant). An increase in friction coefficient was observed on the worn pin surface due to the severe destruction caused by platelet-shaped delaminated wear debris (Fig. 8a–c).

3.4 Tensile strength

Tensile strength and elastic modulus of the AlMg₁SiCu/silicon carbide/molybdenum disulphide hybrid composite are presented in Fig. 9. It is clear from the plot that the tensile strength of hybrid composites increases with the increase in wt.% of MoS₂ particles, but the elastic modulus shows a decreasing trend. One of the reasons for the decrease in the elastic modulus of the hybrid composites is due to the elastic deformation on the grain boundaries. SEM images of the worn-out surfaces (Fig. 7f) show that bonding between coarse particles with longer shallow craters is stronger when

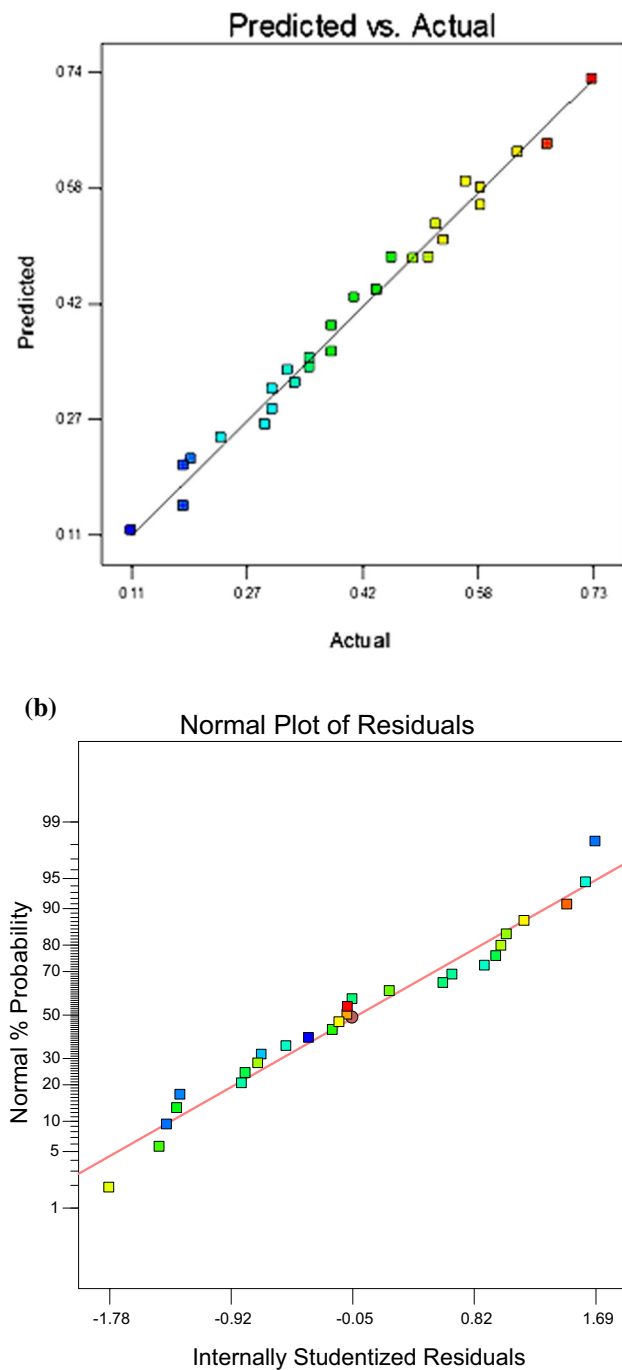


Fig. 12 a Experimental versus predicted values of weight loss (RSM model), b normality plot of residuals for weight loss (RSM model)

compared to finer particles. Increase in the presence of shallow craters and shallow sliding grooves reduce the elastic modulus of the hybrid composites gradually, which leads to increase in tensile strength of the hybrid composites compared to as-cast AlMg1SiCu alloy (Fig. 9) [4]. Maximum tensile strength and minimum elastic modulus were obtained for 10 wt.% SiC and 9 wt.% MoS₂ hybrid composite.

3.5 Mathematical Modelling and ANOVA

The RSM was proposed (Table 3) as the second-order quadratic mathematical model to describe the effect of the input parameters on the weight loss. The mathematical model consists of a constant term, four linear terms and four quadratic terms, and six interaction factors. The effects of these terms of the developed model on the weight loss are stated with positive or negative sign. It was observed that the mathematical equation had a coefficient of determination R square value of 0.98. The R square value can be used to determine if the predicted values were in line with the experimental values.

$$\begin{aligned}
 \text{Wear loss} = & (-0.86571) + (0.095398 * A1) \\
 & + (1.21224E - 3 * B1) + (0.16354 * C1) \\
 & + (1.19337E - 3 * D1) + (1.00000E - 4 * A1 * B1) \\
 & + (5.00000E - 3 * A1 * C1) - (8.33333E - 6 * A1 * D1) \\
 & + (2.63063E - 4 * B1 * C1) - (5.43544E - 7 * B1 * D1) \\
 & - (3.76877E - 5 * C1 * D1) - 0.010195 * A1 * A1 \\
 & - (2.98536E - 6 * B1 * B1) \\
 & - (0.034854 * C1 * C1) \\
 & - (2.06707E - 7 * D1 * D1)
 \end{aligned} \tag{3}$$

ANOVA test was performed to validate statistical significance of the developed model equation. The adequacy of the developed mathematical model as well as the significance of each term in the model was found from the ANOVA results (Table 5). Fischer’s test values (*F*-values) and *p*-values derived from Fischer’s test were used to verify the significance of the models. The associated *F*-values of the developed model were at 95% significance level, according to the ANOVA study. The *F*-values revealed the sufficiency of the model. Furthermore, *p*-value of developed model was lower than 0.05. The findings showed that the above model is capable of predicting weight loss in the range of the variables tested [29].

According to the ANOVA study presented in Table 5, it was observed that the *p*-values of weight fraction of MoS₂, speed, applied load and sliding distance terms obtained from weight loss are lesser than 0.050. These terms indicate that they are important model terms for weight loss in hybrid composites. However, the some of the terms have *p*-values greater than 0.050, indicating that they have a negligible effect on the developed model. Desirability ramp function plot (main effects plots for optimization) for achieving optimum weight loss is shown in Fig. 10, which can be employed to get the optimum weight loss in terms of weight fraction, sliding distance, sliding speed and applied load.

From this plot, an optimum weight loss of 0.146 g could be achieved for weight fraction of 8.999 wt.% of MoS₂,

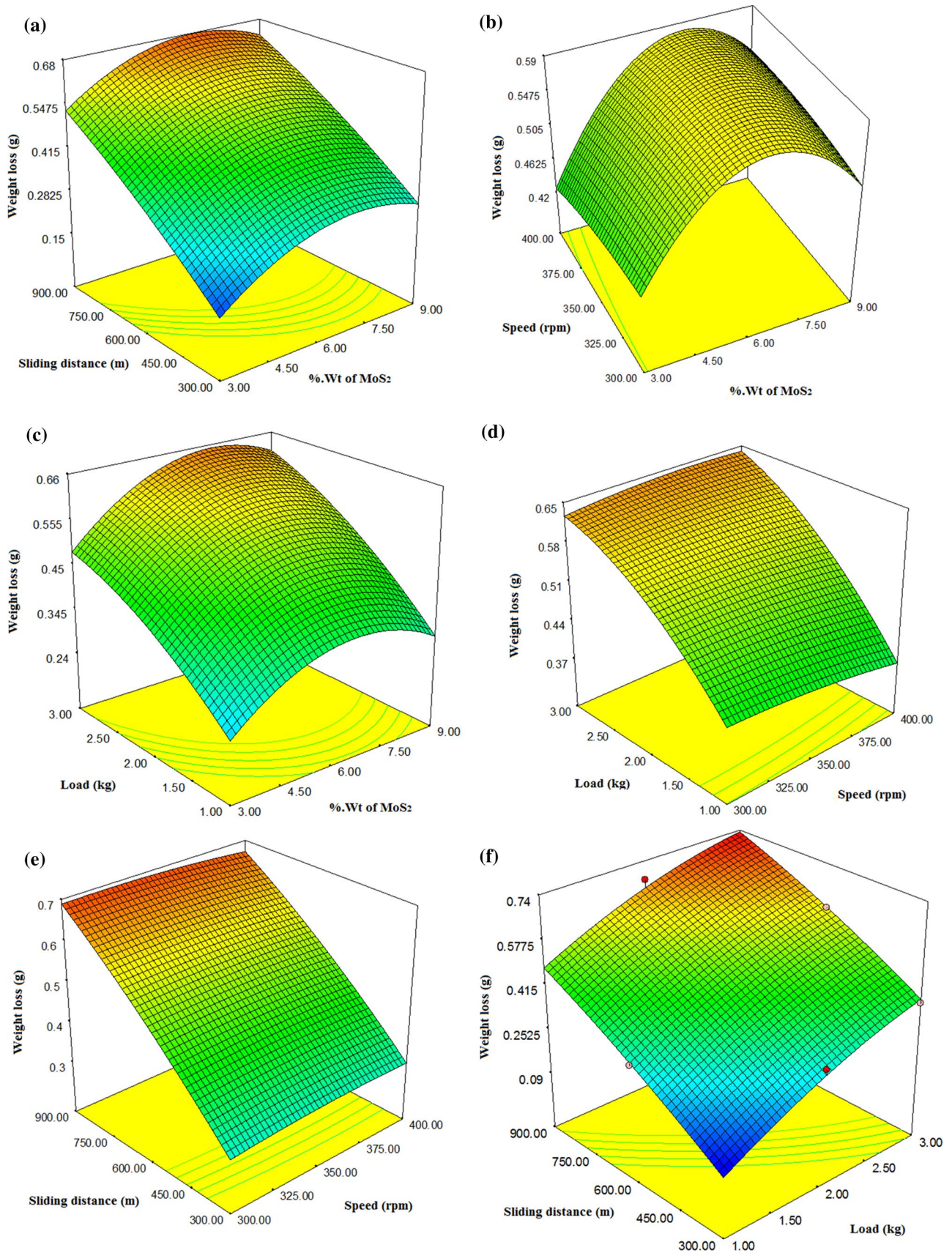


Fig. 13 a-f Surface plots (RSM) for weight loss versus %wt of MoS₂, speed, load and sliding distance



Table 6 ANFIS Training and testing data

Experimen- tal run	wt.% of MoS ₂ (%)	Speed (rpm)	Load (kg)	Sliding dis- tance (m)	Weight loss (g)	
					Experimental	ANFIS
2	3	300	2	300	0.18	0.182
3	3	200	2	600	0.35	0.354
5	3	300	2	900	0.58	0.582
6	3	300	3	600	0.41	0.414
7	6	300	1	300	0.11	0.113
8	6	200	1	600	0.33	0.335
9	6	300	1	900	0.52	0.522
11	6	300	2	600	0.46	0.464
13	6	400	2	300	0.3	0.32
14	6	200	2	900	0.63	0.633
15	6	400	2	900	0.67	0.674
16	6	300	3	900	0.73	0.732
17	6	300	3	300	0.38	0.384
18	6	200	3	600	0.49	0.493
19	6	400	3	600	0.58	0.587
20	6	400	3	300	0.38	0.382
22	9	300	1	600	0.29	0.295
23	9	300	2	300	0.19	0.194
24	9	200	2	600	0.35	0.358
25	9	400	2	600	0.44	0.444
26	9	300	2	900	0.56	0.566
1	3	300	1	600	0.23	0.235
4	3	400	2	600	0.32	0.322
10	6	400	1	600	0.3	0.31
12	6	200	2	300	0.18	0.182
21	6	300	2	600	0.51	0.485
27	9	300	3	600	0.53	0.531

applied load of 1 kg, sliding speed of 221.091 rpm and applied sliding distance of 300.577 m, with a total desirability of 0.920 could be achieved.

Along with wear loss, coefficient of friction (CoF) was also analysed with an aim of minimizing it as it is a measure of reducing the friction between the sliding surfaces. Desirability ramp function plot (main effects plots for optimization) for achieving minimum weight loss and minimum CoF is shown in Fig. 11, which can be employed to get the optimum sliding distance, sliding speed and applied load apart from the predicted values of output. From this plot, an optimum coefficient of friction of 0.233 and optimum weight loss of 0.144 g could be achieved for weight fraction of 8.999 wt.% of MoS₂, applied load of 1 kg, sliding speed of 216.023 rpm and applied sliding distance of 300.108 m, with a total desirability of 0.960 could be achieved. With increase in applied load, the coefficient of friction and weight loss of the composite increases. Coefficient of friction showed a decreasing trend with increasing sliding speed and weight fraction of the MoS₂ reinforcement. The presence of MoS₂

particles significantly reduced the coefficient of friction and weight loss of the AlMg1SiCu alloy hybrid composites.

The comparison between the experimental results and the predicted outputs are shown in Fig. 12. Also, it presents the normality plot on the weight loss of the composites which reveals that the developed model is adequate.

The surface plots (RSM) (Fig. 13a–f) indicate that applied load and sliding distance are the most dominant factors on the magnitude of weight loss of the fabricated hybrid composites. The remaining factors, namely speed and weight fraction of MoS₂, was the least significant when compared to other factors. Figure 13d clearly demonstrates that the applied load has more effect on the weight loss of the hybrid composites. The presence of reinforcement on the fabricated composite Fig. 13a–c confirms that reinforcement wt.% of 9% MoS₂ possess less weight loss when compared with 3% and 6% wt.% MoS₂.



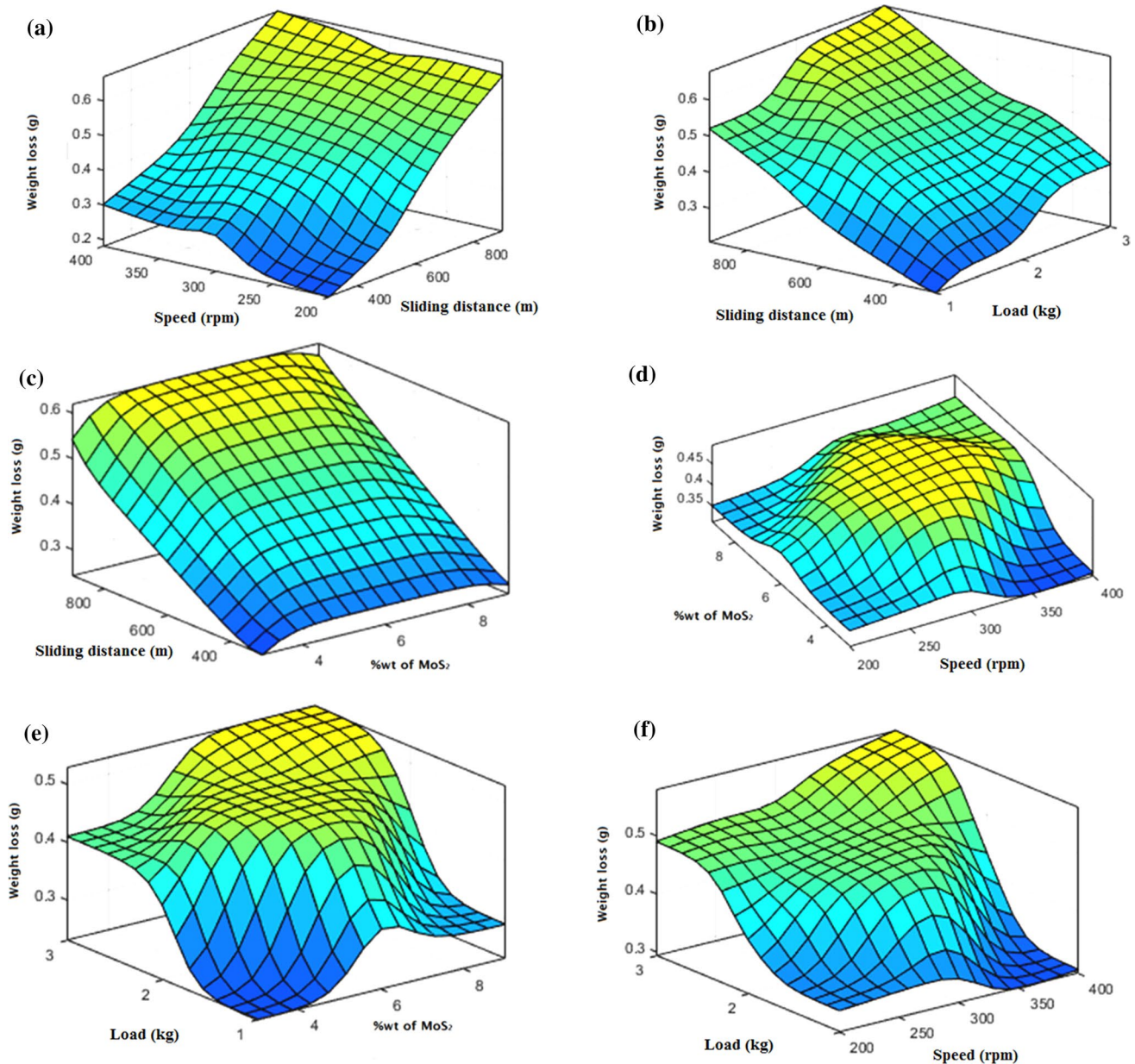


Fig. 14 a–f Surface plots (ANFIS) of weight loss versus %Wt of MoS₂, speed, load and sliding distance

3.6 ANFIS Data Analysis: Prediction-Modelling for Weight Loss

The ANFIS-based prediction model has been developed for weight loss of stir cast AlMg1SiCu/SiC/MoS₂ hybrid metal matrix composite. The input variables with different levels are given in Table 2. A 4-factor-3-level BBD design (Table 3) was employed in these tests. The entire experimental data set was divided into training, testing and checking data sets.

Along with these 27 data sets, 21 sets have been used for training data and remaining 6 sets as testing data. Three

Gaussian type-subclustering membership functions has been selected for input as shown in Fig. 3a and linear type membership function has been used for output during the generation of fuzzy inference system. Then, the accuracy of the proposed model using six set of testing data is presented as shown in Table 6. The developed model structure of ANFIS is shown in Fig. 3b.

ANFIS surface plot analysis on weight loss of the hybrid composites is shown in Fig. 14a–f. From Fig. 14a–c it was found that the applied load and sliding distance were the most dominant factors which influence the weight loss. The weight fraction of MoS₂ and speed were found to have

Table 7 Comparison between RSM and ANFIS results

Statistical parameters	Weight loss (g)	
	RSM	ANFIS
Error prediction		
RMSE	0.000169	1.15741E-05
MAE	0.001852	0.000926
SEP (%)	0.041364	0.002840909
MPE (%)	0.696831	0.190913
R ²	0.98	0.99
χ ²	8.45594E-06	2.10917E-06
Model summary		
Computational time	Short	Long
Experimental domain	Regular	Irregular or regular
Understanding	Easy	Moderate
Model developing	With interactions	No interactions
Application	Frequently	Frequently

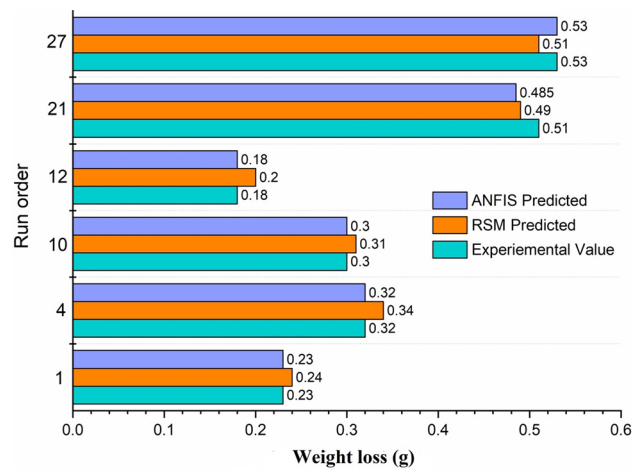


Fig. 16 Comparison between ANFIS, RSM and experimental values of weight loss

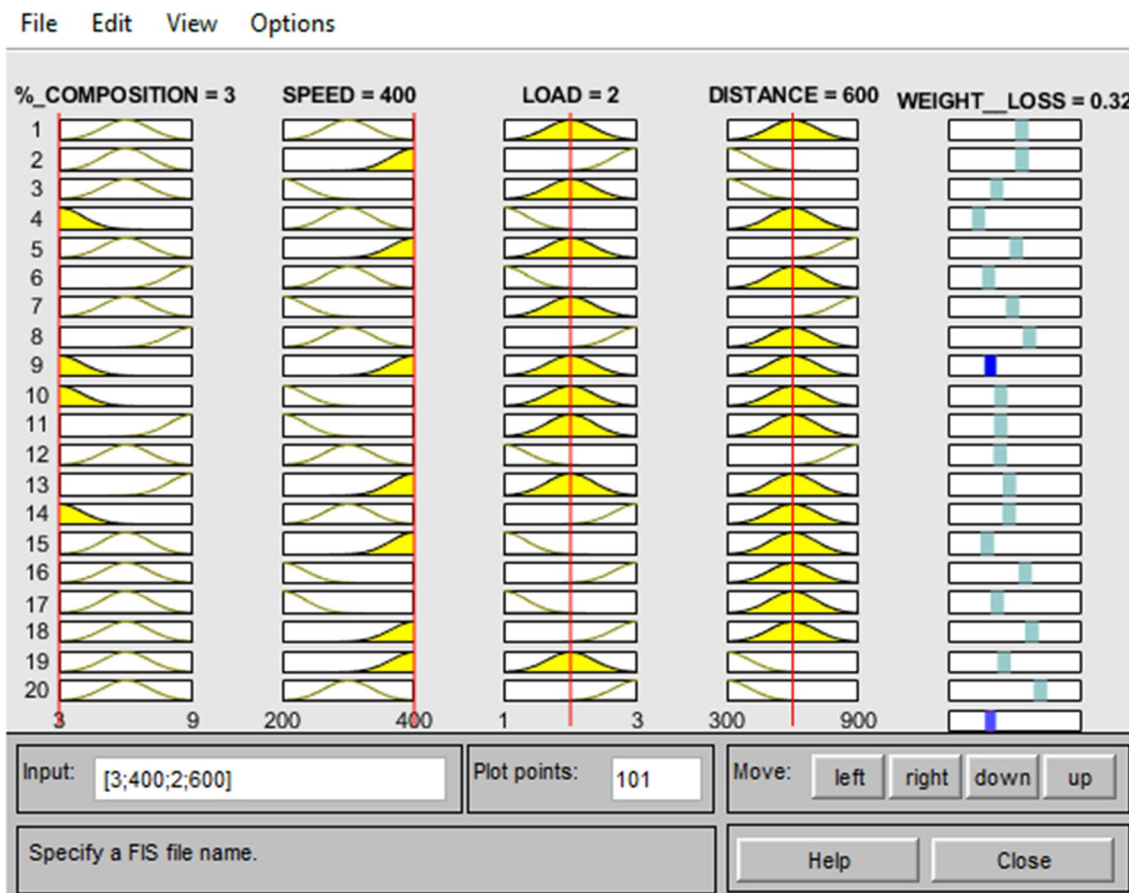


Fig. 15 ANFIS set of rules of testing data for weight loss

less influence on wear of these hybrid composites. From Fig. 14d–e, it was observed that wt.% of 3% MoS₂ and 9% MoS₂ are prone to less wear when compared to 6% MoS₂ weight fraction. This result indicates that up to 9% MoS₂ weight fraction, the hybrid composite exhibits less wear and if increasing gradually up to 6% MoS₂ wt.%, results in high wear. At wt.% of 6% MoS₂, there is a slight drop in weight loss when compared to 9% MoS₂.

The predicted values by ANFIS and RSM models are presented in Table 7. By employing the general statistical analysis, different parameters such as RMSE, MAE, SEP, MPE, coefficient of determination (R^2) and Chi-square statistic (χ^2) has been evaluated by equations in Table 4 to match the results.

A sample set of rules for prediction of wear of the hybrid composites is shown in Fig. 15. The trained ANFIS model was found to be more accurate than the developed RSM model, and hence, it was found from the results that the ANFIS model has superior modelling capability than the RSM model for wear of aluminium reinforced with SiC/MoS₂ composites (Fig. 15). The ANFIS model predictions are found to be much closer to the prediction by RSM model as shown in Fig. 16. Thus, the ANFIS models show a significantly superior generalization capacity than the RSM models. Higher accuracy of prediction by ANFIS was due to its general capability to approximate the nonlinearity of the method, but the RSM is limited to a second-order polynomial.

4 Conclusions

In this study, the effectiveness of RSM and ANFIS models are compared with regard to modelling, prediction and generalization capabilities based on the BBD in the wear prediction of stir casted AlMg1SiCu/SiC/MoS₂ hybrid metal matrix composite. The results acquired are listed as follows:

- As MoS₂ content was increased, the hardness of the hybrid composites improved until 6 wt.% and further addition marginally reduced the hardness.
- It is evident that tensile strength increases with the presence of MoS₂ particles. A maximum tensile strength of 129.76 MPa could be accomplished for 10 wt.% of SiC and 9 wt.% of MoS₂ hybrid composites. Also, maximum strain increased with the addition of MoS₂ solid lubricant.
- Since MoS₂ particles are precipitated along the grain boundaries and they act as nucleus that hinders the growth of α -Al phase, thereby significantly improving the mechanical properties.
- Weight losses of 9% MoS₂ hybrid composite at low sliding speeds were found to be less, with smoother worn-out

pin surface, due to the development of shallow sliding grooves and MoS₂-lubricated tribolayer. However, with the increase in sliding speeds, delamination and abrasion wear could be observed on the worn-out pin surface.

- Coefficient of friction decreased with increasing sliding speed and weight fraction of the MoS₂ reinforcement. The presence of MoS₂ particles significantly reduced the coefficient of friction of the hybrid composites.
- ANOVA results shows that the most significant variables influencing the sliding wear of composites are the applied load, sliding distance and weight fraction of MoS₂, whereas speed proved to possess the least influence on the weight loss of the aluminium hybrid composites.
- The results of the ANFIS model proved that it is more robust in prediction when compared with the RSM models. AlMg1SiCu alloy reinforced with MoS₂ and SiC is found to have superior tribological properties during dry sliding, setting a new guiding principles for the design of materials for relevance to self-lubricating sliding wear conditions.

Funding This research did not receive any specific grant from funding agencies in the public, commercial, or not-for-profit sectors.

Data Availability The raw/processed data required to reproduce these findings cannot be shared at this time as the data also forms part of an ongoing study.

Declarations

Conflict of interest The authors declare that they have no conflict of interest.

References

1. Rao, R.N.; Das, S.: Effect of matrix alloy and influence of SiC particle on the sliding wear characteristics of aluminium alloy composites. *Mater. Design* **31**(3), 1200–1207 (2010). <https://doi.org/10.1016/j.matdes.2009.09.032>
2. Bauri, R.; Surappa, M.K.: Sliding wear behavior of Al–Li–SiC_p composites. *Wear* **265**(11–12), 1756–1766 (2008). <https://doi.org/10.1016/j.wear.2008.04.022>
3. Baradeshwaran, A.; Vettivel, S.C.; Elayapermal, A., et al.: Experimental investigation on mechanical behavior, modelling and optimization of wear parameters of B4C and graphite reinforced aluminium hybrid composites. *Mater. Design* **63**, 620–632 (2014). <https://doi.org/10.1016/j.matdes.2014.06.054>
4. Vinoth, K.S.; Subramanian, R.; Dharmalingam, S., et al.: Mechanical and tribological characteristics of stir-cast Al–Si10Mg and self-lubricating Al–Si10Mg/MoS₂ composites. *Mater. Tech* **46**(5), 497–501 (2012)
5. Menezes, P.L.; Rohatgi, P.K.; Lovel, M.R.: Self-lubricating behaviour of graphite reinforced metal matrix composites. In: Nosonovsk, M.; Bhushan, B. (Eds.) *Green Tribology*, pp. 445–480. Springer, Berlin Heidelberg (2012)



6. Prasad, S.V.; Asthana, R.: Aluminum metal matrix composites for automotive applications; tribological considerations. *Tribol. Lett.* **17**, 445–453 (2004)
7. Dharmalingam, S.; Subramanian, R.; Kök, M.: Optimization of abrasive wear performance in aluminium hybrid metal matrix composites using Taguchi–grey relational analysis. *Proc. Inst. Mech. Eng Part J* **227**, 749–760 (2013)
8. Monikandan, V.V.; Joseph, M.A.; Rajendra Kumar, P.K.: Dry sliding wear studies of aluminum matrix hybrid composites. *Res. Effi. Technol.* **2**, S12–S24 (2016)
9. Deuis, R.L.; Subramanian, C.; Yellup, J.M.: Dry sliding wear of aluminum composites—a review. *Compos. Sci. Technol.* **57**, 415–435 (1997)
10. Sahoo, P.; Ghosh, S.: Tribological behavior of aluminium metal matrix composites—a review. *J. Tribol. Res* **2**(1), 1–14 (2011)
11. Sahin, Y.: The prediction of wear resistance model for the metal matrix composites. *Wear* **258**(11–12), 1717–1722 (2005). <https://doi.org/10.1016/j.wear.2004.11.024>
12. Velmurugan, C.; Subramanian, R.; Thirugnanam, S.: Experimental study on the effect of SiC and graphite particles on weight loss of Al 6061 hybrid composite materials. *J. Tribol. Surf. Eng* **2**(1–2), 49–68 (2011)
13. Kumar, S.; Balasubramanian, V.: Effect of reinforcement size and volume fraction on the abrasive wear behaviour of AA7075 Al/SiC_p/P/M composites—a statistical analysis. *Tribol. Int.* **43**(1–2), 414–422 (2010). <https://doi.org/10.1016/j.triboint.2009.07.003>
14. Suresh, S.; Shenbaga-Vinayaga-Moorthi, N.; Vettivel, S.C., et al.: Mechanical behavior and wear prediction of stir cast Al–TiB₂ composites using response surface methodology. *Mater. Design* **59**, 383–396 (2014). <https://doi.org/10.1016/j.matdes.2014.02.053>
15. Manjunath-Patel, G.C.; Krishna, P.; Parapagoundar, B.M.: Squeeze casting process modeling by a conventional statistical regression analysis approach. *Appl. Math. Model* **40**(15–16), 6869–6888 (2016). <https://doi.org/10.1016/j.apm.2016.02.029>
16. Vijayakumar, S.; Karunamoorthy, L.: Modelling wear behaviour of Al–SiC metal matrix composites: soft computing technique. *Tribol. Mater. Surf. Interfaces* **6**, 25–30 (2013). <https://doi.org/10.1179/1751584X12Y.0000000002>
17. Velmurugan, C.; Muthukumar, V.; Ragupathy, K., et al.: Modelling Volume loss of heat treated Al6061 composites using ANN. *Proced. Mater. Sci* **5**, 31–40 (2014). <https://doi.org/10.1016/j.mspro.2014.07.239>
18. Gajalakshmi, K.; Senthilkumar, N.; Prabu, B.: Multi-response optimization of dry sliding wear parameters of AA6026 using hybrid gray relational analysis coupled with response surface method. *Meas. Cont.* **52**(5–6), 540–553 (2019). <https://doi.org/10.1177/0020294019842603>
19. Hashim, J.; Looney, L.; Hashmi, M.S.J.: Particle distribution in cast metal matrix composites—part II. *J. Mater. Proc. Technol.* **123**, 258–263 (2002). [https://doi.org/10.1016/S0924-0136\(02\)00099-7](https://doi.org/10.1016/S0924-0136(02)00099-7)
20. Lu, J.; Lu, Z.: Optimization of stirring parameters through numerical simulation for the preparation of aluminum matrix composite by stir casting process. *J. Manuf. Sci. Eng.* **132**(061007), 1–7 (2010). <https://doi.org/10.1115/1.4002851>
21. Sahin, Y.: Tribological behaviour of metal matrix and its composite. *Mater. Des.* **28**, 1348–1352 (2007)
22. Rebba, B.; Ramanaiah, N.: Evaluation of mechanical properties of aluminium alloy (Al–2024) reinforced with molybdenum disulphide (MoS₂) metal matrix composites. *Procedia Mater Sci* **6**, 1161–1169 (2014). <https://doi.org/10.1016/j.mspro.2014.07.189>
23. Sun, C.; Song, M.; Wang, Z.; He, Y.: Effect of particle size on the microstructures and mechanical properties of SiC-reinforced pure aluminum composites. *J. Mater. Eng. Perf.* **20**, 1606–1612 (2016)
24. Koker, R.; Altinkok, N.; Demir, A.: Neural network-based prediction of mechanical properties of particulate reinforced metal matrix composites using various training algorithms. *Mater. Design* **28**(2), 616–627 (2007)
25. Sannino, A.P.; Rack, H.J.: Surface topography evolution during sliding wear of 2009 Al–SiCp/17–4 PH. *Wear* **181–183**, 202–211 (1995)
26. Velmurugan, C.; Subramanian, R.; Thirugnanam, S., et al.: Investigation of friction and wear behavior of hybrid aluminium composites. *Ind. Lub. Trib* **64**(3), 152 (2012). <https://doi.org/10.1108/00368791211218687>
27. Gopalakrishnan, S.; Murugan, N.: Production and wear characterization of AA 6061 matrix titanium carbide particulate reinforced composite by enhanced stir casting method. *Comp. Part B* **43**(2), 302–308 (2012). <https://doi.org/10.1016/j.compositesb.2011.08.049>
28. Rajesh, S.; Velmurugan, C.; Ebenezer Jacob Dhas, D.S.; Samuel Ratna Kumar, P.S.: Studies on the tribological behaviour of exsitu-synthesized AlMg1SiCu/titanium carbide/molybdenum disulfide hybrid composites. *Mater. Res. Express* **6**, 1264 (2019). <https://doi.org/10.1088/2053-1591/ab5f1e>
29. Manjunath-Patel, G.C.; Shettigar, A.K.; Mahesh-Parappagoudar, B.: A systematic approach to model and optimize wear behaviour of castings produced by squeeze casting process. *J. Manuf. Proc* **32**, 199–212 (2018). <https://doi.org/10.1016/j.jmapro.2018.02.004>
30. Mandal, N.; Roy, H.; Mondal, B.; Murmu, N.; Mukhopadhyay, S.: Mathematical modeling of wear characteristics of 6061 Al–alloy–SiCp composite using response surface methodology. *J. Mater. Eng. Perform.* **21**, 17–24 (2012). <https://doi.org/10.1007/s11665-011-9890-7>
31. Hamidreza, G.; Mohd, H.I.; Norhayati, A.; Navid, M.: Microstructure development mechanical and tribological properties of a semisolid A356/xSiCp composite. *J. Appl. Res. Technol.* **15**, 533–544 (2017). <https://doi.org/10.1016/j.jart.2017.06.002>
32. Kanthavel, K.; Sumesh, K.R.; Saravanakumar, P.: Study of tribological properties on Al/Al₂O₃/MoS₂ hybrid composite processed by powder metallurgy. *Alexan. Eng. J.* **55**, 13–17 (2016). <https://doi.org/10.1016/j.aej.2016.01.024>

